Available online at www.sciencedirect.com
SCIENCE DIRECT®
ELSEVIER
International Journal of Solids and Structures 43 (2006) 5066–5084
INTERNATIONAL JOURNAL OF SOLIDS and STRUCTURES
www.elsevier.com/locate/ijsolstr

Refined models of elastic beams undergoing large in-plane motions: Theory and experiment

Walter Lacarbonara [a,*], Hiroshi Yabuno [b]

[a] *Dipartimento di Ingegneria Strutturale e Geotecnica, Università di Roma La Sapienza, via Eudossiana 18, Rome 00184, Italy*
[b] *Institute of Engineering Mechanics and Systems, University of Tsukuba, Tsukuba-City 305-8573, Japan*

Received 14 April 2005; received in revised form 5 July 2005
Available online 1 September 2005

Abstract

Accurate mechanical models of elastic beams undergoing large in-plane motions are discussed theoretically and experimentally. Employing the geometrically exact theory of rods with appropriate kinematic assumptions and asymptotic arguments, two approximate models are obtained—a relaxed model and its constrained version—that describe extensional and bending motions and neglect shear deformations. These models are shown to be suitable to predict, via an asymptotic approach, closed-form nonlinear motions of beams with general boundary conditions and, in particular, with boundary conditions that longitudinally constrain the motions. On the other hand, for axially unrestrained or weakly restrained beams, an inextensible and unshearable model is presented that describes bending motions only. The perturbations about the reference configuration up to third order are consistently derived for all beam models. Closed-form solutions of the responses to primary-resonance excitations are obtained via an asymptotic treatment of the governing equations of motion for two different beam configurations; namely, hinged–hinged (axially restrained) and simply supported (axially unrestrained) beams. In particular, considering the present theory and the existing theories, variations of the frequency–response curves with the beam slenderness or the relative boundary mass are investigated for the lowest modes. The fidelity of the proposed nonlinear models is ascertained comparing the theoretically obtained frequency–response curves of the first mode with those experimentally obtained.

Keywords: Nonlinear beam; Axis stretching nonlinearity; Finite bending curvature; Geometric/inertia nonlinearities; Direct method of multiple scales

* Corresponding author. Tel.: +39 06 44585293; fax: +39 06 4884852.
E-mail address: walter.lacarbonara@uniroma1.it (W. Lacarbonara).

0020-7683/$ - see front matter © 2005 Elsevier Ltd. All rights reserved.
doi:10.1016/j.ijsolstr.2005.07.018

1. Introduction

Large-amplitude planar motions of beam structures are encountered in a variety of engineering applications. These motions are excited around resonances with finite displacements and rotations whereas the strains often remain small.

The most comprehensive theory today available to describe overall motions of rods is the *special Cosserat theory* of rods (Villaggio, 1997). The beam is mathematically conceived as a one-dimensional continuum with a local rigid structure. Because of the postulated local rigidity, the sections cannot undergo distortion and warping deformations; therefore, the theory is mainly restricted to beams with closed cross-sections.

In the literature, there have been various implementations of the special Cosserat theory of rods. In particular, in computational mechanics, different finite element formulations have been presented to address either nonlinear statics or overall motions of rods in space. Beside numerical approaches, analytical treatments, often based on perturbation techniques, have been used to address static and dynamic problems (Eisley, 1964; Atluri, 1973; Nayfeh et al., 1974; Crespo da Silva and Glynn, 1978; Luongo et al., 1986; Nayfeh and Pai, 2004; Lacarbonara et al., 2004). A few works have compared the solutions obtained via finite element schemes with those analytically obtained such as for cables undergoing resonant motions (Gattulli et al., 2004).

Typically, the analytical approaches have employed approximate mechanical models that account for geometric and inertia nonlinearities, often using a variational formulation based on a truncated kinematic model. Restricting the attention to planar shear-undeformable beams, there are two main groups of works. One is devoted to studying hinged–hinged (axially restrained) beams considering the hardening effect of the beam axis stretching as dominant nonlinearity. These studies (Eisley, 1964; Nayfeh et al., 1974; Lacarbonara and Camillacci, 2004) have been mostly inspired by the work due to Mettler (1962).

A few other works have dealt with modeling of the dynamic behavior of beams without axial restraints whereby the most important nonlinearities have been singled out in the nonlinear inertia forces and finite bending curvature (Atluri, 1973; Crespo da Silva and Glynn, 1978). In particular, Atluri (1973) was the first to recognize the intrinsically different nonlinear signatures of the beams of the first group in contrast with those of the second group. Namely, he showed that the first mode of beams without axial restraints exhibits a softening nonlinearity in contrast with that of axially restrained beams that are of the hardening type and concluded that longitudinal inertia is the dominant nonlinearity in the first case.

Later, Luongo et al. (1986) revisited this problem in a unified fashion. Considering two truncated kinematic models and employing Hamilton's extended principle, they investigated the nonlinear features of the beams of the two groups with different boundary conditions. They considered the first and third modes and confirmed the results obtained by Atluri (1973). Crespo da Silva (1988) derived a model accounting for stretching, curvature and inertia nonlinearities and showed that the stretching effect is dominant for axially restrained beams.

Beside the widespread nature of these studies, there seems to be a lack of mathematical consistency in the way the truncated mechanical models of nonlinear beams are obtained—often based on ad hoc kinematic approximations—as well as a lack of experimental validation of the fidelity of the ensuing models. Hence, the primary objective of the present work is to obtain rigorously and systematically approximate mechanical models that accurately describe finite planar motions of beams with general boundary conditions and to compare their leading predictions with experimental results. Moreover, it is of interest to compare the theoretical results obtained via the proposed models with those obtained using Mettler's theory applicable to axially restrained beams. To this end, we investigate variations of the effective nonlinearity coefficient of the lowest modes as it regulates the qualitative character of the nonlinear frequency–response functions—softening-type versus hardening-type behavior —as well as the quantitative dependence of the mode nonlinear frequency corrections on the oscillation amplitude.

The paper is organized as follows. The geometrically exact equations of motion, without a priori kinematic approximations, are discussed in Section 2. The second perturbation of the governing equations of motion for general beams is presented in Section 2.1. In Sections 3 and 4, two beam models are considered, namely, a constrained model for extensible beams and a model for inextensible beams. In Section 5, the asymptotic solutions are obtained applying directly the method of multiple scales to the equations governing the two beam configurations—axially restrained and unrestrained beams—subject to a primary resonance of an arbitrary bending mode. The main analytical predictions, relating to the different nonlinear signatures—softening versus hardening—of the first mode of hinged–hinged (axially restrained) and simply supported (axially unrestrained) beams are discussed also with reference to previously adopted beam models. In Section 6, the main experimental results are presented and the theoretically obtained frequency–response curves are compared with those experimentally obtained. In Section 7, the concluding remarks are drawn.

2. Mechanical formulation for elastic beams undergoing large in-plane motions

In this section, the kinematics and mechanics describing overall planar motions of elastic beams are summarized. The beam is straight in its *rest reference configuration* $\mathscr{C}_n$ (Fig. 1); it is sufficiently slender with a closed cross-section and is made of a hyperelastic and homogeneous material. Due to its relatively high slenderness, the beam is considered absolutely unshearable.

A Lagrangian description of the motion is adopted. Denoting with $\mathbf{e}_j$ $(j = 1,2,3)$ the orthonormal vectors of a fixed inertial reference frame (Fig. 1, bottom) such that $\mathbf{e}_1$ is parallel to the beam base curve (here, coincident with the beam undeformed centroidal axis), the position of a material point along the beam axis is represented by the vector $\mathbf{X}(x) := x\mathbf{e}_1$ where x denotes the coordinate along the straight undeformed beam axis with the origin O fixed at the left end. Thus, the elastodynamic problem becomes parameterized with x spanning the compact support $D := \{x | x \in [0, \ell]\}$, where ℓ is the length of the undeformed beam axis in $\mathscr{C}_n$. The generic material section in the reference configuration $\mathscr{C}_n$ is specified by the pair of orthonormal vectors $\mathbf{a}_2$ and $\mathbf{a}_3$, $\mathbf{a}_1 := \mathbf{a}_2 \times \mathbf{a}_3$ is set so that $(\mathbf{a}_1, \mathbf{a}_2, \mathbf{a}_3)$ is a right-handed orthonormal basis in $\mathbb{E}^3$ Euclidean space. Due to time-dependent in-plane forces, acting in the $(\mathbf{e}_1, \mathbf{e}_2)$-plane, represented by body forces $\mathbf{b}(x,t)$ and couples $\mathbf{c}(x,t) := c(x,t)\mathbf{e}_3$ per unit reference length, boundary forces $\mathbf{B}(t)$ and couples $\mathbf{C}(t)$ applied on the free boundary, the beam undergoes a naturally planar deformation process in the $(\mathbf{e}_1, \mathbf{e}_2)$-plane, a plane of symmetry for the beam.

Denoting the displacement vector from $\mathscr{C}_n$ to $\mathscr{C}$ with $\mathbf{u} := u\mathbf{a}_1 + v\mathbf{a}_2$, the section placement is then defined by the position vector $\mathbf{x}(x,t) := \mathbf{X}(x) + \mathbf{u}(x,t)$ and by the pair of orthonormal directors $\mathbf{d}_2(x,t)$ and $\mathbf{d}_3(x,t)$, respectively (again, $\mathbf{d}_1 := \mathbf{d}_2 \times \mathbf{d}_3$). The directors $\mathbf{d}_j$ $(j = 1,2)$ are obtained from $\mathbf{a}_j$ via a finite rotation about

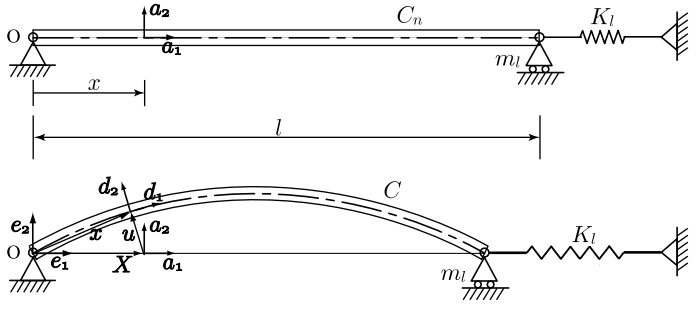

Fig. 1. Scheme of the beam with the end mass and spring in the rest (top) and current (bottom) configurations, respectively.

the $\mathbf{d}_3$-axis, described by the proper orthogonal rotation tensor $\mathbf{R}(x,t)$, restricted to the plane spanned by $\mathbf{a}_1$ and $\mathbf{a}_2$; that is, $\mathbf{d}_j = \mathbf{R}\mathbf{a}_j$ with $\mathbf{R}\mathbf{e}_1 := [\cos\theta, \sin\theta]^\top$ and $\mathbf{R}\mathbf{e}_2 := [-\sin\theta, \cos\theta]^\top$ where use of the matrix notation has been made and $\top$ indicates the transpose.

The beam generalized strains are calculated in the reference configuration as the components of the following *strain vector* and *curvature tensor*, respectively. Namely, the strain vector is defined as $\boldsymbol{\epsilon}(x,t) := \mathbf{R}^\top\mathbf{x}' - \mathbf{X}'$ and the curvature tensor is $\mathbf{K}(x,t) := \mathbf{R}^\top\mathbf{R}'$ where the prime denotes differentiation with respect to x.

The beam unshearability is enforced via the internal kinematic constraint $\gamma := \boldsymbol{\epsilon}\cdot\mathbf{a}_2 = 0$ (the dot indicates the standard dot product in $\mathbb{E}^2$ Euclidean space). This constraint, in turn, is solved to yield the beam section rotation as

$$\theta = \tan^{-1}\left(\frac{v'}{1+u'}\right) \tag{1}$$

where $\tan^{-1}$ denotes the inverse of the tangent function. Furthermore, $\sin\theta = v'/(1+\varepsilon)$ and $\cos\theta = (1+u')/(1+\varepsilon)$. Consequently, the only nontrivial strains are the *axial strain* and the *bending curvature*, the non-zero component of the curvature tensor $\mathbf{K}$, and are expressed as

$$\varepsilon := \boldsymbol{\epsilon}\cdot\mathbf{a}_1 \equiv \sqrt{(1+u')^2 + (v')^2} - 1 \quad \text{and} \quad k := \theta' \equiv \frac{v''+u'v''-u''v'}{(1+\varepsilon)^2} \tag{2}$$

Let the contact force and couple, mutually exerted by two adjoining sections, be expressed as

$$\mathbf{n}(x,t) := N(x,t)\mathbf{d}_1(x,t) + H(x,t)\mathbf{d}_2(x,t), \quad \mathbf{m}(x,t) := M(x,t)\mathbf{d}_3 \tag{3}$$

where N and H indicate the axial load and shear force, respectively, and M is the bending moment. The equilibrium equations, requiring the balance of linear momentum and moment of momentum, are

$$\mathbf{n}' + \mathbf{b} = \mathbf{0} \tag{4}$$

$$M' + \mathbf{d}_3\cdot(\mathbf{x}'\times\mathbf{n}) + c = 0 \tag{5}$$

where $\times$ denotes the vector product. Beside the kinematic boundary conditions that prescribe $\mathbf{u}$ and θ, the mechanical boundary conditions are

$$N\mathbf{d}_1 + H\mathbf{d}_2 = \mp\mathbf{B}, \quad \mathbf{m} = \mp\mathbf{C} \tag{6}$$

where the minus and plus signs refer to $x = 0$ and $x = \ell$, respectively. The equilibrium equations, after filtering out the shear force H, become

$$N' + \frac{k}{1+\varepsilon}M' + \frac{k}{1+\varepsilon}c + b_1 = 0 \tag{7}$$

$$\left(\frac{M'}{1+\varepsilon}\right)' + \left(\frac{c}{1+\varepsilon}\right)' - kN - b_2 = 0 \tag{8}$$

where $b_1(x,t)$ and $b_2(x,t)$ denote the body forces per unit reference length along the $\mathbf{d}_1$ and $\mathbf{d}_2$ directions, respectively.

By virtue of D'Alembert's principle, we can express the external body forces, the dissipative viscous forces and the inertia forces and the corresponding couples in the form $\mathbf{b}(x,t) := \mathbf{f} - \mathbf{f}_d - \rho A\ddot{\mathbf{x}} = (f_1 - c_u\dot{u} - \rho A\ddot{u})\mathbf{a}_1 + (f_2 - c_v\dot{v} - \rho A\ddot{v})\mathbf{a}_2$ and $\mathbf{c}(x,t) := (c_e - c_\theta\dot{\theta} - \rho I\ddot{\theta})\mathbf{a}_3$ where $\dot{\theta}$ and $\ddot{\theta}$ are obtained differentiating (2) with respect to time t, ρ is the mass density; A is the area of the cross-section; I denotes the moment of inertia about the $\mathbf{a}_3$-axis which is one of the principal inertia axes of the beam cross-section; c_u, c_v and c_θ denote the linear viscous damping coefficients in the directions indicated by the subscript;

c_e is the density of the external couples; and the overdot indicates differentiation with respect to time t. To inertially uncouple the equations of motion, we project them into the $(\mathbf{a}_1, \mathbf{a}_2)$-basis and obtain

$$\rho A\ddot{u} + c_u\dot{u} - \left[N' + \frac{k}{1+\varepsilon}M' + \frac{k}{1+\varepsilon}(c_e - c_\theta\dot{\theta} - \rho I\ddot{\theta})\right]\cos\theta - \left[\left(\frac{M'}{1+\varepsilon}\right)' - kN + \left(\frac{c_e - c_\theta\dot{\theta} - \rho I\ddot{\theta}}{1+\varepsilon}\right)'\right]\sin\theta = f_1 \tag{9}$$

$$\rho A\ddot{v} + c_v\dot{v} - \left[N' + \frac{k}{1+\varepsilon}M' + \frac{k}{1+\varepsilon}(c_e - c_\theta\dot{\theta} - \rho I\ddot{\theta})\right]\sin\theta + \left[\left(\frac{M'}{1+\varepsilon}\right)' - kN + \left(\frac{c_e - c_\theta\dot{\theta} - \rho I\ddot{\theta}}{1+\varepsilon}\right)'\right]\cos\theta = f_2 \tag{10}$$

Considering the boundary conditions of the beam in Fig. 1, they are expressed as

$$u(0,t) = 0, \quad v(0,t) = 0, \quad v(\ell,t) = 0, \quad M(0,t) = M(\ell,t) = 0 \tag{11}$$

$$N\cos\theta + \frac{M'}{1+\varepsilon}\sin\theta = -m_\ell\ddot{u} - K_\ell u \quad \text{at } x = \ell \tag{12}$$

where m_ℓ and K_ℓ are the lumped mass and the end spring constant (see Fig. 1).

The presence of an end load, $P(t)$, applied onto the roller support would render the boundary conditions nonhomogeneous. In Section 3, discussing a constrained model for extensible beams, it will be clear that the governing equations of motion can be lumped into an integral–partial–differential equation with time-varying coefficients arising from the time-varying boundary action. This indicates that, beside primary and secondary (super- or sub-harmonic, combination) resonances, also parametric resonances may occur and simultaneously internal resonances may be initiated due to the nonlinear modal coupling forces.

From a constitutive point of view, the material is hyperelastic, isotropic and homogeneous. Moreover, because (i) the axial strain is small, (ii) the curvature is moderately large and (iii) the selected base curve is the centroidal curve, then the constitutive equations are assumed in the linearized and uncoupled form

$$N(x,t) = EA(x)\varepsilon(x,t), \quad M(x,t) = EI(x)k(x,t) \tag{13}$$

where E indicates Young's modulus.

2.1. Perturbed equations of motion

In view of seeking asymptotically valid solutions for moderately large-amplitude motions, the geometrically exact equations of motion are perturbed around the reference configuration $\mathscr{C}_n$ by considering their Mac Laurin series expansions up to third polynomial order. To this end, the axial strain and bending curvature are first expanded as

$$\varepsilon(x,t) \approx u' + \frac{1}{2}(v')^2 - \frac{1}{2}u'(v')^2, \quad k(x,t) \approx v'' - (u'v')' - v'^2v'' + (u'^2v')' \tag{14}$$

Substituting these expressions into the constitutive laws, Eq. (13), the ensuing internal forces are further substituted into the equations of motion (9) and (10). Their subsequent expansions to third order yield the governing equations of motion that, neglecting the small rotary inertia and damping rotary terms and the external couples, can be written as

$$\rho A\ddot{u} + c_u\dot{u} - (EAu')' - \frac{1}{2}(EAv'^2)' + \left[(EAu')v'^2\right]' - \left[(EIv'')'v'\right]' + \left\{\left[EI(u'v')'\right]'v'\right\}' + 2\left[(EIv'')'(u'v')\right]' = f_1 \tag{15}$$

$$\rho A\ddot{v} + c_v\dot{v} + (EIv'')'' - \left[(EIv'')'u'\right]' - \left[EI(u'v')'\right]'' + \left\{\left[EI(u'v')'\right]'u'\right\}' + \left[(EIv'')'(u'^2 - v'^2)\right]' + \left[EI(u'^2v')'\right]'' - \left[EIv'^2v''\right]'' - (EAu'v')' + (EAu'^2v')' - \frac{1}{2}\left(EAv'^3\right)' = f_2 \tag{16}$$

Similarly, the expansion of the mechanical boundary conditions, Eqs. $(11)_4$ and (12), gives

$$EI\left[v'' - (u'v')' - v'^2v'' + (u'^2v')'\right] = 0 \tag{17}$$

$$m_\ell\ddot{u} + K_\ell u + EAu' + \frac{1}{2}EAv'^2 - EAu'v'^2 + (EIv'')'v' - (EIv'')'u'v' - \left[EI(u'v')'\right]'v' = 0 \tag{18}$$

In the literature, it has been a common practice to derive the governing equations of motion using Hamilton's extended principle (Crespo da Silva and Glynn, 1978; Luongo et al., 1986; Nayfeh and Pai, 2004) which reads $\delta\mathscr{H}^* = \int_{t_1}^{t_2}[\delta(T-U) + \delta W]\,\mathrm{d}t = 0$ where T and U indicate the kinetic and potential energies, respectively, and δW denotes the virtual work performed by the distributed forces $Q_u := f_1 - c_u\dot{u}$ and $Q_v := f_2 - c_v\dot{v}$. Of course, adopting the kinematical model whose strains are described by (14), and employing Hamilton's extended principle, the same equations of motion, (15) and (16), and boundary conditions, (17) and (18), are obtained via the variational process. Retaining terms up to fourth order in the energies, the kinetic and strain energies are, respectively,

$$T = \frac{1}{2}\int_0^\ell \rho A\left(\dot{u}^2 + \dot{v}^2\right)\mathrm{d}x + \frac{1}{2}m_\ell\dot{u}(\ell,t)^2 \tag{19}$$

$$U = \frac{1}{2}\int_0^\ell EA\left[u'^2 + u'v'^2 - u'^2v'^2 + \frac{1}{4}v'^4\right]\mathrm{d}x + \frac{1}{2}\int_0^\ell EI\left[v''^2 - 2(u''v'v'' + u'v''^2) + v'^2u''^2 + 6u'u''v'v'' + 3u'^2v''^2 - 2v'^2v''^2\right]\mathrm{d}x + \frac{1}{2}K_\ell u(\ell,t)^2 \tag{20}$$

Considering the boundary condition (18), depending on the magnitude of $\mu := m_\ell/(\rho A\ell)$ or $k_\ell := (\ell^3K_\ell)/(EI)$, the beam may behave quite differently. When $\mu \gg 1$ and/or $k_\ell \gg 1$, the end reaction force acts to restrict the motion of the beam boundary. Consequently, the beam axis may be subject to extensions. In the limit of an infinitely large spring constant or mass, the right boundary condition becomes that of an immovable hinge.

On the other hand, when $\mu = \mathrm{O}(1)$ and $k_\ell = \mathrm{O}(1)$ or they are infinitesimal, the axial motion at the boundary is weakly constrained, and, hence, if there are no applied loads in the longitudinal direction, the beam practically behaves as an inextensible medium. Of course, the general equations of motion (15) and (16) hold in both scenarios, although when the axial deformation is truly negligible, a kinematically constrained model is preferable from a computational standpoint. In the next section, we discuss the derivation of a constrained model whereby the longitudinal motion is expressed in terms of the leading transverse motion. Then, in Section 4, an accurate model for inextensible beams is presented.

3. A constrained model for extensible beams

It is assumed that there are no longitudinal loads (i.e., $b_1 \equiv 0$) so that the longitudinal inertia force can be considered of higher order with respect to the other axial forces. We further assume that the rotary inertia

and damping terms and the distributed couples are negligible. Integrating the balance equation in the $\mathbf{d}_1$-direction, Eq. (7), from ℓ to x and incorporating the mechanical boundary condition (12) yields

$$N(x,t) = -\left[\frac{M'}{1+\varepsilon}\tan\theta + \sec\theta(m_\ell \ddot{u} + K_\ell u)\right]\Big|_{x=\ell} - \int_\ell^x kM'\,\mathrm{d}z - \int_\ell^x b_1\,\mathrm{d}z \tag{21}$$

Therefore, substituting (21) into (8) yields

$$\frac{M''}{1+\varepsilon} - \frac{\varepsilon'}{(1+\varepsilon)^2}M' + k\left[\frac{M'}{1+\varepsilon}\tan\theta + \sec\theta(m_\ell \ddot{u} + K_\ell u)\right]\Big|_{x=\ell} + k\int_\ell^x kM'\,\mathrm{d}z + k\int_\ell^x b_1\,\mathrm{d}z - b_2 = 0 \tag{22}$$

To express the longitudinal motion in terms of the transverse motion only, we solve $(2)_1$ with respect to u', then expand the result, discard higher-order terms, and obtain

$$u' = -1 \pm \sqrt{(1+\varepsilon)^2 - v'^2} \approx -\frac{1}{2}v'^2 + \varepsilon \equiv -\frac{1}{2}v'^2 + \frac{N}{EA} \tag{23}$$

where use of the constitutive law, $\varepsilon = N/(EA)$, has been made. Further, it is necessary to determine how the axial load depends on the leading transverse motion. To this end, a second-order expansion of N is sought so as to have terms of like order in Eq. (23). The inertial force contributing to N can be expressed as $b_{1I} = -\rho A(\ddot{u} + \ddot{v}v') + \cdots \approx -\rho A \ddot{v}v'$ where the assumption that $|\ddot{u}| = \mathrm{o}(|\ddot{v}v'|)$ has been made based on the fact that, in absence of resonant external axial loads, the longitudinal acceleration is indeed small. Therefore, considering consistently the longitudinal boundary acceleration of higher order and substituting the second-order expansion of N into (23) yields

$$u' = -\frac{1}{2}v'^2 - \frac{1}{EA}\left[(EIv'')'v' + K_\ell u\right]\Big|_{x=\ell} + \frac{1}{EA}\left[\int_\ell^x \rho A \ddot{v}v'\,\mathrm{d}z - \int_\ell^x v''(EIv'')'\,\mathrm{d}z\right] \tag{24}$$

whose integration, on account of $u(0,t) = 0$, gives the longitudinal motion. The boundary axial motion $u(l,t)$ can then be calculated as

$$\begin{aligned} u(l,t) = -\left(1 + K_\ell\int_0^\ell \frac{1}{EA}\,\mathrm{d}x\right)^{-1}\Bigg\{&\frac{1}{2}\int_0^\ell v'^2\,\mathrm{d}x + \left[v'(EIv'')'\right]\Big|_{x=\ell}\int_0^\ell \frac{1}{EA}\,\mathrm{d}x \\ &- \int_0^\ell \frac{1}{EA}\left[\int_\ell^x \rho A\ddot{v}v'\,\mathrm{d}z - \int_\ell^x v''(EIv'')'\,\mathrm{d}z\right]\mathrm{d}x\Bigg\} \end{aligned} \tag{25}$$

Accounting for the computed u' and u'', the third-order curvature can then be expressed as

$$k = v'' + \frac{1}{2}v'^2 v'' - \left\{\frac{v'}{EA}\left[\int_\ell^x \rho A\ddot{v}v'\,\mathrm{d}z - \int_\ell^x v''(EIv'')'\,\mathrm{d}z\right]\right\}' + \left(\frac{v'}{EA}\right)'\left[v'(EIv'')' + K_\ell u\right]\big|_{x=\ell} \tag{26}$$

where $u(\ell,t)$ is given by (25). Substituting (26) into the constitutive law (13), and the result into (22), yields the governing equation of motion as

$$\begin{aligned} &\rho A\left(\ddot{v} - \frac{1}{2}\ddot{v}v'^2 - \ddot{u}v'\right) - v''\int_\ell^x \rho A(\ddot{u} + \ddot{v}v')\,\mathrm{d}z - \left[\frac{(EIv'')'}{EA}\int_\ell^x \rho A\ddot{v}v'\,\mathrm{d}z\right]' - \left\{EI\left[\frac{v'}{EA}\int_\ell^x \rho A\ddot{v}v'\,\mathrm{d}z\right]'\right\}'' \\ &+ v''m_\ell\ddot{u}_\ell + (EIv'')'' + \frac{1}{2}\left[EIv'^2v''\right]'' + \left[\frac{(EIv'')'}{EA}\int_\ell^x (EIv'')'v''\,\mathrm{d}z\right]' - \left\{EI\left[\frac{v'}{EA}\int_\ell^x (EIv'')'v''\,\mathrm{d}z\right]'\right\}'' \\ &+ v''\int_\ell^x (EIv'')'v''\,\mathrm{d}z + \left[K_\ell u + (EIv'')'v'\right]\big|_{x=\ell}\left\{v'' + \left[EI\left(\frac{v'}{EA}\right)'\right]'' + \left[\frac{(EIv'')'}{EA}\right]'\right\} = f_2 \end{aligned} \tag{27}$$

where $\ddot{u}(x,t)$ and $\ddot{u}_\ell(t)$ are obtained differentiating, twice with respect to time, the longitudinal motion resulting from (24) and (25). The dissipative forces have not been included for conciseness.

3.1. Equation of motion according to Mettler

The case of immovable or nearly immovable boundaries could be obtained as the limit case of the elastically constrained beam when the end spring stiffness becomes relatively high. In this limit process, it is reasonable to consider inertia and curvature nonlinearities of higher order as a consequence of the longitudinally constrained nature of the resulting motions. In fact, letting the spring constant approach infinity, in agreement with Crespo da Silva (1988), the limit spring reaction force becomes

$$K_\ell u(l,t) = -\frac{EA}{2\ell}\int_0^\ell v'^2\,\mathrm{d}x \tag{28}$$

Therefore, assuming uniform cross-section properties and using (28), the governing equation of motion leads to

$$\rho\ddot{v} + EIv'''' - \frac{EA}{2\ell}v''\int_0^\ell v'^2\,\mathrm{d}x = f_2 \tag{29}$$

which is the equation first proposed by Mettler (1962).

4. A mechanical formulation for inextensible beams

When the beam is axially unrestrained or weakly restrained, it is reasonable and, computationally convenient, to enforce vanishing of the axis elongation, $\varepsilon = 0$, which leads to

$$\Lambda(u',v') := (1+u')^2 + (v')^2 - 1 = 0 \tag{30}$$

Solving (30) with respect to u' yields $u' = -1 \pm (1-(v')^2)^{(1/2)}$. The expansion of u' in a Mac Laurin series gives, to within second order, $u' \approx -1/2(v')^2$ and, consequently, using the kinematic boundary condition $u(0,t) = 0$ gives the longitudinal motion along with the associated velocity and acceleration. On account of $\varepsilon = 0$, the exact bending curvature, $k(x) = \theta'(x)$, and its third-order expansion become

$$k := v'' + u'v'' - u''v' \approx v'' + \frac{1}{2}(v')^2 v'' \tag{31}$$

Moreover, $\sin\theta = v'$ and $\cos\theta \approx 1 + u' \approx 1 - 1/2(v')^2$.

The balance equations are (7) and (8) with $\varepsilon = 0$; further, the mechanical boundary condition in the axial direction at $x = \ell$ is given by (12) with $\varepsilon = 0$. Therefore, the axial force is given by Eq. (21) with $\varepsilon = 0$. The balance equation in the transverse direction becomes

$$M'' + k[M'\tan\theta + \sec\theta(m_\ell\ddot{u} + K_\ell u)]|_{x=\ell} + k\int_\ell^x kM'\,\mathrm{d}z + k\int_\ell^x b_1\,\mathrm{d}z - b_2 = 0 \tag{32}$$

Incorporating the longitudinal motion into the inertial forces, substituting them into (32), expanding the resulting equation and retaining terms up to third order yields the following equation of motion:

$$\rho A\left\{\ddot{v}+v'\int_0^x\left[(\dot{v}')^2+v'\ddot{v}'\right]\mathrm{d}z-\frac{1}{2}\ddot{v}(v')^2\right\}+v''\int_\ell^x\rho A\left[-v'\ddot{v}+\int_0^x(\dot{v}'^2+v'\ddot{v}')\,\mathrm{d}z\right]\mathrm{d}x$$
$$-m_\ell v''\int_0^\ell(\dot{v}'^2+v'\ddot{v}')\,\mathrm{d}x+v''\left\{\left[(EIv'')'v'\right]\big|_{x=\ell}-\frac{1}{2}K_\ell\int_0^\ell(v')^2\,\mathrm{d}x\right\}+\left[EI\left(v''+\frac{1}{2}(v')^2v''\right)\right]''$$
$$+v''\int_\ell^x v''(EIv'')'\,\mathrm{d}z=f_2(x,t) \tag{33}$$

The remaining mechanical boundary conditions (Fig. 1), to within third order, are

$$EI\left[v''+\frac{1}{2}(v')^2v''\right]=0,\quad \text{at } x=0,\ell \tag{34}$$

Also in this case, Hamilton's extended principle can be effectively employed to obtain the equations of motion. The inextensibility constraint is added to the Hamiltonian via a Lagrange multiplier; its minimization leads to

$$\delta\mathscr{H}^*=\int_{t_1}^{t_2}\left\{\delta(T-U)+\delta W+\frac{1}{2}\delta\int_0^\ell\gamma\Lambda(u',v')\,\mathrm{d}x\right\}\mathrm{d}t=0 \tag{35}$$

where Λ indicates the inextensibility constraint (30) and γ is the Lagrange multiplier. The kinetic and strain energies are, respectively, given by (19) and

$$U=\frac{1}{2}\int_0^\ell EI\left[v''^2+2u'v''^2-2v'v''u''\right]\mathrm{d}x+\frac{1}{2}K_\ell u(\ell,t)^2 \tag{36}$$

Previously proposed models of inextensible beams (Crespo da Silva and Glynn, 1978; Luongo et al., 1986) were based on the adoption of different truncated energies.

5. Asymptotic solutions

In this section, asymptotic expansions of the responses of both axially restrained and unrestrained uniform beams subject to primary-resonance excitations are sought employing the method of multiple scales directly applied to the partial-differential equation of motion and boundary conditions (Lacarbonara, 1999). First, we discuss the general relaxed solution for axially restrained beams and, then, the axially unrestrained case.

5.1. Extensible beams

A suitable non-dimensional form of (15) and (16) and of the boundary conditions can be obtained by introducing the following nondimensional variables and parameters:

$$t^*:=\omega_c t,\quad x^*:=\frac{x}{\ell},\quad v^*:=\frac{v}{l},\quad \lambda^2:=\frac{EA}{EI}\ell^2,\quad \mu:=\frac{m_\ell}{\rho A\ell},\quad k_\ell:=\frac{\ell^3K_\ell}{EI} \tag{37}$$

where $\omega_c^2:=(EI)/(\rho A\ell^4)$. The resulting nondimensional equations of motion, dropping the star for sake of notational simplicity and neglecting the rotary inertia and rotary damping terms along with the distributed couples, are

$$\ddot{u}+c_1\dot{u}-\lambda^2\left(u''+v'v''-v'^2u''-2u'v'v''\right)-v''v'''-v'v''''+2u''v''^2+4v'v''u'''+5v'u''v'''+3u'v''v''''$$
$$+v'^2u''''+3u'v'v''''=p_1(x,t) \tag{38}$$

$$\ddot{v} + c_2\dot{v} + v'''' - \lambda^2\left(v'u'' + u'v'' - 2u'v'u'' - u'^2v'' + \frac{3}{2}v'^2v''\right) - 3v''u''' - v'u'''' - 2u'v'''' - 4u''v''' + 7v'u''u''' + 8u''^2v'' - 2v''^3 + 9u'v''u''' + 12u'u''v''' - 8v'v''v''' + 3u'v'u'''' + \left(3u'^2 - 2v'^2\right)v'''' = p_2(x,t) \tag{39}$$

where c_1, c_2 and p_1, p_2 are the nondimensional damping coefficients and external force components in the axial and transverse directions, respectively.

We consider a harmonic uniform base acceleration near the primary resonance of the nth bending mode away from internal resonances with any other mode. The associated distributed force is $f_2 := -\rho A\ddot{y}_b^*$ and its nondimensional form is $p_2 := a_b\omega^{*2}\cos\omega^* t$ where $\omega^* := \omega/\omega_c$ and $a_b := Y_b/\ell$ (ω and Y_b are the dimensional circular frequency and amplitude of the prescribed base displacement). For the beam shown in Fig. 1, the nondimensional mechanical boundary conditions are

$$v'' - (u'v')' - (v')^2v'' + (u'^2v')' = 0, \quad \text{at } x = 0, 1 \tag{40}$$

$$\mu\ddot{u} + k_\ell u + \lambda^2\left(u' + \frac{1}{2}(v')^2 - u'(v')^2\right) + v'''v' - u'v'v''' - \left[(u'v')'\right]'v' = 0, \quad \text{at } x = 1 \tag{41}$$

Due to the axially constrained nature of the motions (when k_ℓ and/or μ are large), the longitudinal motion is of higher order with respect to the transverse motion; then, uniform expansions of the solutions of (38) and (39) are sought in the form

$$\begin{aligned} u(x,t) &= \epsilon^2 u_2(x, T_0, T_2) + \cdots \\ v(x,t) &= \epsilon v_1(x, T_0, T_2) + \epsilon^3 v_3(x, T_0, T_2) + \cdots \end{aligned} \tag{42}$$

where ϵ is a small nondimensional ordering parameter and $T_j := \epsilon^j t$, $j = 0, 2$, are the governing unstretched and stretched time scales, respectively. The time derivatives can then be expressed in terms of the independent time scales as $\partial/\partial t \approx D_0 + \epsilon^2 D_2$ and $\partial^2/\partial t^2 \approx D_0^2 + 2\epsilon^2 D_0 D_2$, with $D_j := \partial/\partial T_j$. Moreover, the excitation and dissipative forces are demoted to third order where the internal and external resonant forces can balance each other.

Substituting (42) into the governing equations of motion (38) and (39) and equating like powers of ϵ to zero yields

Order ϵ:

$$D_0^2 v_1 + v_1'''' = 0 \tag{43}$$

Order ϵ^2:

$$D_0^2 u_2 - \lambda^2 u_2'' = \lambda^2 v_1' v_1'' + v_1'' v_1''' + v_1' v_1'''' \tag{44}$$

Order ϵ^3:

$$D_0^2 v_3 + v_3'''' = -D_2 v_1 - 2\zeta D_0 v_1 + \lambda^2 v_1' u_2'' + \frac{3}{2}\lambda^2 v_1'^2 v_1'' + 3v_1'' u_2''' + v_1' u_2'''' + 2u_2' v_1'''' + 4u_2'' v_1''' + 2v_1''^3 + 8v_1' v_1'' v_1''' + 2v_1'^2 v_1'''' + \left(\frac{1}{2}a_b\omega^2 e^{i\omega T_0} + \text{cc}\right) \tag{45}$$

where ζ is the damping ratio in the transverse direction and cc indicates the complex conjugate of the preceding terms.

Because $\omega \approx \omega_n$, the nth bending mode is directly excited at resonance, and because there are no internal resonances involving this mode with any other mode so that energy transfer between the modes cannot occur, we assume the solution at order ϵ as

$$v_1 = A_n(T_2)\mathrm{e}^{\mathrm{i}\omega_n T_0}\phi_n(x) + \mathrm{cc} \tag{46}$$

where $(\omega_n, \phi_n(x))$ is the nth eigenpair (natural frequency, mode shape). Due to the self-adjointeness of the linear unforced undamped problem, the eigenfunctions ϕ_m are mutually orthogonal and they are normalized as follows $\int_0^1 \phi_m\phi_n\,\mathrm{d}x = \delta_{mn}$ with δ_{mn} denoting the Kronecker delta.

The second-order problem and its particular solution are, respectively, given by

$$D_0^2 u_2 - \lambda^2 u_2'' = (A_n\overline{A}_n + A_n^2\mathrm{e}^{2\mathrm{i}\omega_n T_0})\left[\lambda^2\phi_n'\phi_n'' + \phi_n''\phi_n''' + \phi_n'\phi_n''''\right] + \mathrm{cc} \tag{47}$$

$$u_2 = A_n\overline{A}_n\psi_1(x) + A_n^2\mathrm{e}^{2\mathrm{i}\omega_n T_0}\psi_2(x) + \mathrm{cc} \tag{48}$$

where the overbar indicates the complex conjugate and the functions $\psi_j(x)$ are solutions of the following boundary-value problems:

$$\lambda^2\psi_1'' = -(\lambda^2\phi_n'\phi_n'' + \phi_n''\phi_n''' + \phi_n'\phi_n'''') \tag{49}$$

$$\lambda^2\psi_2'' + 4\omega_n^2\psi_2 = -(\lambda^2\phi_n'\phi_n'' + \phi_n''\phi_n''' + \phi_n'\phi_n'''') \tag{50}$$

with the associated boundary conditions on ψ_j.

Substituting v_1 and u_2 into the third-order problem and imposing thereafter its solvability yields

$$2\mathrm{i}\omega_n(\dot{A} + \zeta A) = \Gamma_n A_n^2\overline{A}_n + \frac{1}{2}a_b\mathrm{e}^{\mathrm{i}\sigma t} \tag{51}$$

where the resonance detuning condition, $\omega = \omega_n + \epsilon^2\sigma$, $\sigma \in \mathbb{R}$, has been used. Further solving for the fixed points of the real-valued modulation equations resulting from (51), the following frequency–response equation is obtained:

$$\omega = \omega_n - \Gamma_n a^2 \pm \sqrt{\left(\frac{a_b}{2\omega_n a}\right)^2 - \zeta^2} \tag{52}$$

where a is the amplitude of the motion at leading order. The *effective nonlinearity coefficient* Γ_n in (52) can be expressed as $\Gamma_n = \Gamma_n^{(u)} + \Gamma_n^{(v)}$ with

$$\begin{aligned}\Gamma_n^{(u)} = {} & \lambda^2\left[2\int_0^1 \psi_1''\phi_n'\phi_n\,\mathrm{d}x + \int_0^1 \psi_2''\phi_n'\phi_n\,\mathrm{d}x + 2\int_0^1 \psi_1'\phi_n''\phi_n\,\mathrm{d}x + \int_0^1 \psi_2'\phi_n''\phi_n\,\mathrm{d}x\right] \\ & + 3\left(2\int_0^1 \psi_1'''\phi_n''\phi_n\,\mathrm{d}x + \int_0^1 \psi_2'''\phi_n''\phi_n\,\mathrm{d}x\right) + 2\int_0^1 \psi_1''''\phi_n'\phi_n\,\mathrm{d}x + \int_0^1 \psi_2''''\phi_n'\phi_n\,\mathrm{d}x \\ & + 2\left(2\int_0^1 \psi_1'\phi_n''''\phi_n\,\mathrm{d}x + \int_0^1 \psi_2'\phi_n''''\phi_n\,\mathrm{d}x\right) + 4\left(2\int_0^1 \psi_1''\phi_n'''\phi_n\,\mathrm{d}x + \int_0^1 \psi_2''\phi_n'''\phi_n\,\mathrm{d}x\right)\end{aligned} \tag{53}$$

$$\Gamma_n^{(v)} = \frac{9}{2}\lambda^2\int_0^1 \phi_n''(\phi_n')^2\phi_n\,\mathrm{d}x + 6\int_0^1 (\phi_n'')^3\phi_n\,\mathrm{d}x + 24\int_0^1 \phi_n'\phi_n''\phi_n'''\phi_n + 6\int_0^1 (\phi_n')^2\phi_n''''\phi_n\,\mathrm{d}x \tag{54}$$

The coefficient $\Gamma_n^{(u)}$ captures contributions from the longitudinal motion via the functions ψ_j whereas $\Gamma_n^{(v)}$ relates to effects of the transverse motion. For a hinged–hinged uniform beam, the eigenpair is $\omega_n = n^2\pi^2$ and $\phi_n = \sqrt{2}\sin n\pi x$, $n = 1,2,\ldots$. The functions $\psi_j(x)$, solutions of the boundary-value problems (49) and (50) with boundary conditions $\psi_j(0) = \psi_j(1) = 0$ (hinged–hinged beam), can be expressed as

$$\psi_1(x) = -\frac{1}{4}n\pi\left(1 - 2\frac{n^2\pi^2}{\lambda^2}\right)\sin 2n\pi x, \quad \psi_2(x) = -\frac{n\pi(2n^2\pi^2 - \lambda^2)}{4(n^2\pi^2 - \lambda^2)}\sin 2n\pi x \tag{55}$$

The computations leading to the effective nonlinearity coefficient resulted in

$$\Gamma_n^{(u)} = \frac{1}{4}n^4\pi^4\frac{(2n^2\pi^2 - 3\lambda^2)(2n^2\pi^2 - \lambda^2)^2}{\lambda^2(n^2\pi^2 - \lambda^2)}, \quad \Gamma_n^{(v)} = \frac{3}{4}n^4\pi^4(6n^2\pi^2 - 3\lambda^2) \tag{56}$$

On the other hand, using Mettler's theory, Eq. (29), yields the effective nonlinearity coefficient $\Gamma_n^{\mathrm{M}} = -3/2\lambda^2 n^4\pi^4$.

Next, we discuss the main analytical predictions with emphasis on comparing the results obtained with the proposed theory with those obtained using Mettler's theory. To this end, we observe that the frequency–response curves, given by Eq. (52), exhibit a softening- or hardening-type behavior depending on whether Γ_n is positive or negative. Beside regulating the qualitative character of the nonlinear frequency–response functions, this coefficient also affects quantitatively the dependence of the mode nonlinear frequency corrections on the oscillation amplitude. Therefore, we closely investigate this coefficient.

It is convenient to refer to the nondimensional properties of the test beam used in the experiments reported in Table 1. In Fig. 2, we show a typical frequency–response curve when $\lambda = 1948$, $\zeta = 0.06$, and $a_b = 1.2\times10^{-5}$. The calculated effective nonlinearity coefficient is $\Gamma_1 = -5.548\times10^8$ and is the summation of $\Gamma_1^{(u)} = 2.77\times10^8$ and $\Gamma_1^{(v)} = -8.32\times10^8$. The fact that $\Gamma_1^{(u)} > 0$ entails that the contribution from the longitudinal motion is of the softening type. However, because $\Gamma_1 < 0$, the resulting frequency–response curve is of the hardening type. Analyzing Eq. (56) allows to conclude that all modes are of the hardening type for all physically admissible slendernesses (i.e., $\lambda \geqslant 30$).

We note that the effective nonlinearity coefficient, for very slender beams (i.e., $\lambda^2 \to \infty$), converges to that obtained with Mettler's theory. Therefore, we can conclude that Mettler's solution converges asymptotically to the actual solution, within the range of moderately large oscillation amplitudes, for rather slender beams whose effective axial stiffness is much larger than the bending stiffness thus making the stretching geometric nonlinearity the dominant nonlinearity. However, for non-slender beams, the discrepancies may become significant as it is shown in Fig. 3 where variation of the percent difference in the effective nonlinearity coefficients obtained with the two models is shown when varying λ. We further note that (i) the difference increases with the mode number and/or for small slenderness and (ii) the effective nonlinearity coefficient obtained using Mettler's theory may overestimate the actual coefficient by as much as 70% for the fifth mode of non-slender beams or between 5% and 40% for lower modes. For completeness, mention must be made of the fact that, for non-slender beams, the model should be further relaxed and allow also shear deformations.

To look closely into the differences between the theories, we calculated the axial strains employing Mettler's theory and the proposed theory and obtained, respectively,

$$\varepsilon(t) = \frac{1}{2}a^2(1 + \cos 2(\omega t + \gamma_n))\int_0^1 (\phi_n')^2\,\mathrm{d}x \tag{57}$$

Table 1
Properties of the test beam

Length (mm)	450
Width (mm)	10
Thickness (mm)	0.8
Density (kg/m^3)	8890
Young modulus (GPa)	116

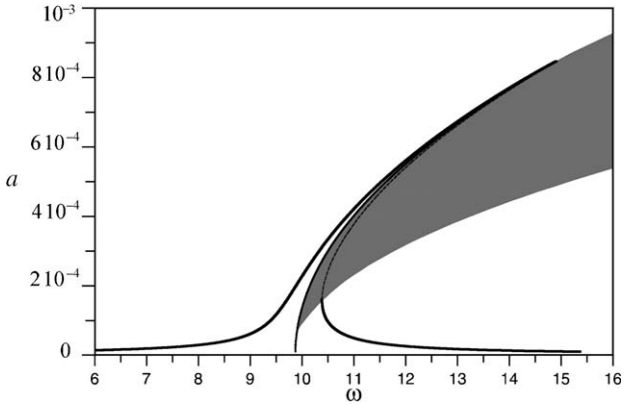

Fig. 2. Frequency–response curve of the first mode of a hinged–hinged beam with $\lambda = 1948$, $\zeta = 0.06$, and $a_b = 1.2 \times 10^{-5}$. The dashed region indicates unstable solutions (saddles).

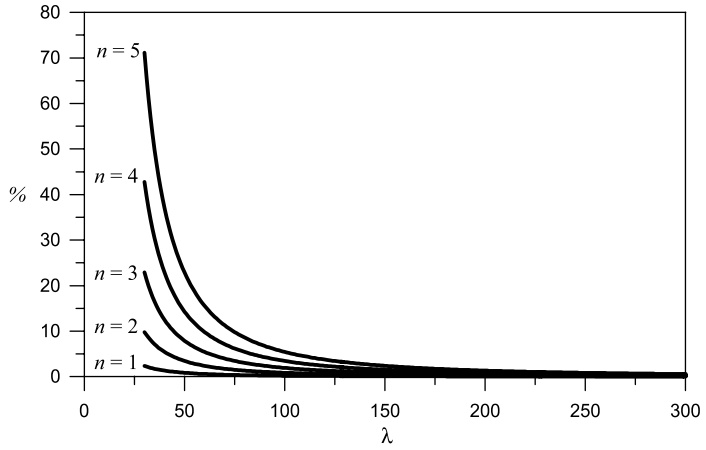

Fig. 3. Variation with the slenderness λ of the percent relative difference of the effective nonlinearity coefficient obtained with Mettler's theory with respect to the relaxed theory for the lowest five modes of a hinged–hinged beam.

$$\varepsilon(x,t) = \frac{1}{2}a^2\left[(\psi_1' + \frac{1}{2}\phi_n'^2) + (\psi_2' + \frac{1}{2}\phi_n'^2)\cos 2(\omega t + \gamma_n)\right] \tag{58}$$

We note that the strain calculated via Mettler's theory is uniform and turns out to be an average of the actual strain (58) which, on the other hand, exhibits a variation along the beam span with a number of half waves that is twice the number associated with the excited mode shape. This strain variation is governed by the functions ψ_j and the mode shape and induces a stretching effect that, overall, is smaller than that predicted by the more constrained Mettler's theory.

5.2. Inextensible beams

The governing equation of motion for inextensible beams is given by (33). Asymptotic solutions are obtained applying the method of multiple scales directly to (33). Using the general results reported in

Lacarbonara and Camillacci (2004), the frequency–response equation is again given by Eq. (52) where the effective nonlinearity coefficient is now expressed as $\Gamma_n = 3\Gamma_n^{\mathrm{G}} + \Gamma_n^{\mathrm{I}}$ with

$$\Gamma_n^{\mathrm{G}} = -\left[\phi_n'''\phi_n'\big|_{x=1} - \frac{1}{2}k_\ell\int_0^1(\phi_n')^2\,\mathrm{d}x\right]\int_0^1\phi_n''\phi_n\,\mathrm{d}x - \frac{1}{2}\int_0^1\phi_n\left[(\phi_n')^2\phi_n''\right]''\mathrm{d}x - \int_0^1\left(\phi_n''\phi_n\int_1^x\phi_n''\phi_n'''\,\mathrm{d}z\right)\mathrm{d}x \tag{59}$$

$$\Gamma_n^{\mathrm{I}} = \omega_n^2\left[\mu\int_0^1\phi_n''\phi_n\,\mathrm{d}x\int_0^1(\phi_n')^2\,\mathrm{d}x - \int_0^1\left(\phi_n'\phi_n\int_0^x(\phi_n')^2\,\mathrm{d}z\right)\mathrm{d}x - \int_0^1\left(\phi_n''\phi_n\int_1^x\int_0^z(\phi_n')^2\,\mathrm{d}y\,\mathrm{d}z\right)\mathrm{d}x\right] - 3\omega_n^2\left[\mu\left(\int_0^1\phi_n''\phi_n\,\mathrm{d}x\right)\left(\int_0^1(\phi_n')^2\,\mathrm{d}x\right) - \int_0^1\left(\phi_n'\phi_n\int_0^x(\phi_n')^2\,\mathrm{d}z\right)\mathrm{d}x + \int_0^1\left(\phi_n''\phi_n\int_1^x\phi_n'\phi_n\,\mathrm{d}z\right)\mathrm{d}x - \int_0^1\left(\phi_n''\phi_n\int_1^x\int_0^z(\phi_n')^2\,\mathrm{d}y\,\mathrm{d}z\right)\mathrm{d}x\right] \tag{60}$$

Here, Γ_n^{G} relates to the contribution from the geometric and curvature nonlinearities whereas Γ_n^{I} is the contribution arising from the nonlinear inertia forces. The result of the calculations for the simply-supported beam shown in Fig. 1 is

$$\Gamma_n^{\mathrm{G}} = -\frac{3}{2}n^4\pi^4(k_\ell + 3n^2\pi^2), \quad \Gamma_n^{\mathrm{I}} = n^6\pi^6\left[\frac{19}{8} + \frac{1}{3}n^2\pi^2(1+6\mu)\right] \tag{61}$$

Calculating the effective nonlinearity coefficient for the same test beam ($\lambda = 1948$ and $\mu = 8.1$) yields $\Gamma_1 = 1.55\times10^5$ with $\Gamma_1^{\mathrm{G}} = -4326$ and $\Gamma_1^{\mathrm{I}} = 1.59\times10^5$. The frequency–response curve corresponding to $\zeta = 0.06$ and $a_b = 1.1\times10^{-3}$ is shown in Fig. 4. As expected, due to the dominating inertia nonlinearity, the curve is of the softening type. On the other hand, using the approximate theory described in Luongo et al. (1986), the effective nonlinearity coefficient becomes

$$\Gamma_n = \frac{n^6\pi^6}{12}(8n^2\pi^2 - 45) - \frac{3}{2}k_\ell n^4\pi^4 + 2n^8\pi^8\mu \tag{62}$$

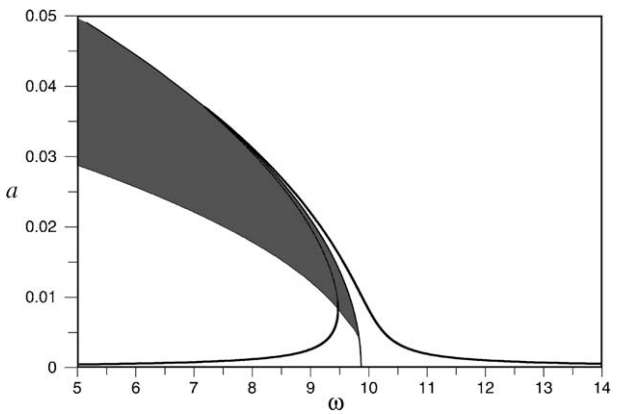

Fig. 4. Frequency–response curve of the first mode of a simply supported (axially unrestrained) beam with $\lambda = 1948$, $\zeta = 0.06$, $\mu = 8.1$, and $a_b = 1.1\times10^{-3}$. The dashed region indicates unstable solutions (saddles).

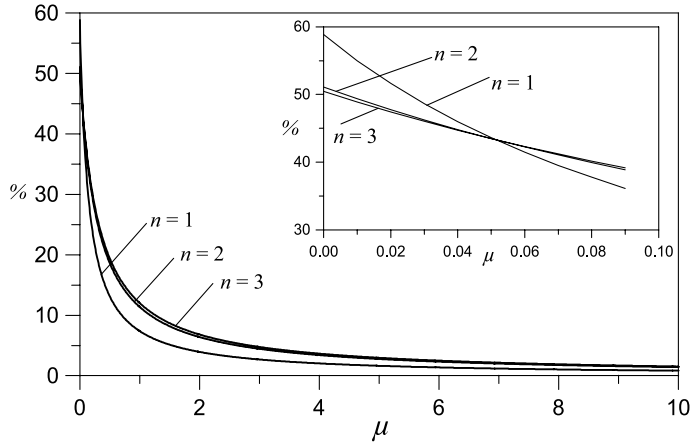

Fig. 5. Variation with the mass ratio μ of the percent relative difference of the effective nonlinearity coefficient obtained with the existing theory, Eq. (62), with respect to the proposed model for the lowest three modes of a simply supported beam.

It is interesting to calculate the percent relative difference in the effective nonlinearity coefficient obtained with the proposed theory, Eq. (61), and with the existing theory, Eq. (62). As shown in Fig. 5, it is clear that (i) Eq. (62) overestimates the effective nonlinearity coefficient with an increasing rate for smaller mass ratios and can be as much as 50% and (ii) except for rather small mass ratios, the difference increases for higher modes.

6. Experimental results and comparison with the theory

The experimental setup, shown in Fig. 6, consists of the test specimen and the base whose sinusoidal displacement is controlled by an electromagnetic shaker (EMIC: 371-A, maximum excitation force of 98 N). The test specimen is a uniform beam with rectangular cross-section made of phosphore bronze ($450 \times 10 \times 0.8$ mm^3), which is supported by hinges made of radial bearings (JIS 6200). One of the hinges is rigidly clamped onto the base. The other hinge is mounted on top of a sliding linear bearing (IKO Ball Slide Unit, Model BSU 44-50 A) to realize the axially movable end. When the sliding linear bearing is mechanically locked, the beam ends are both hinged and immovable. Two laser sensors were used to measure the displacements of the beam and the base excitation, respectively: a KEYENCE LB-01 (resolution of 40 μm and sampling time of 20 ms) and a KEYENCE LC-2430 (resolution of 0.02 μm and a sampling time of 20 ms). Also, a strain gauge was attached to the midspan of the beam to measure the strains in the simply supported (axially movable) configuration.

To generate frequency–response curves, we monitored the time traces and frequency contents of the displacements and strains of the beam by using a portable signal analyzer (ONO SOKKI: DS2100).

We preliminarily measured the first natural frequency (6.47 Hz) and the logarithmic decrement for estimating the damping ratio from the time history of the free response of the mid-span section in Fig. 7. We found $\delta = 0.3659$ and $\zeta = 0.06$, respectively. Then, considering the same excitation amplitude as that in Fig. 3 ($Y_b = 0.017$ mm), we performed forward and backward frequency sweeps around the first natural frequency to construct the frequency–response curves. The experimentally obtained frequency–response curve is superimposed on the theoretically obtained curve in Fig. 8. The filled (unfilled) circles indicate the forward (backward) sweeps. The arrows indicate the jumps. As expected, the first mode is of the hardening type. The fact that the downward jump occurs at a lower amplitude than that theoretically predicated

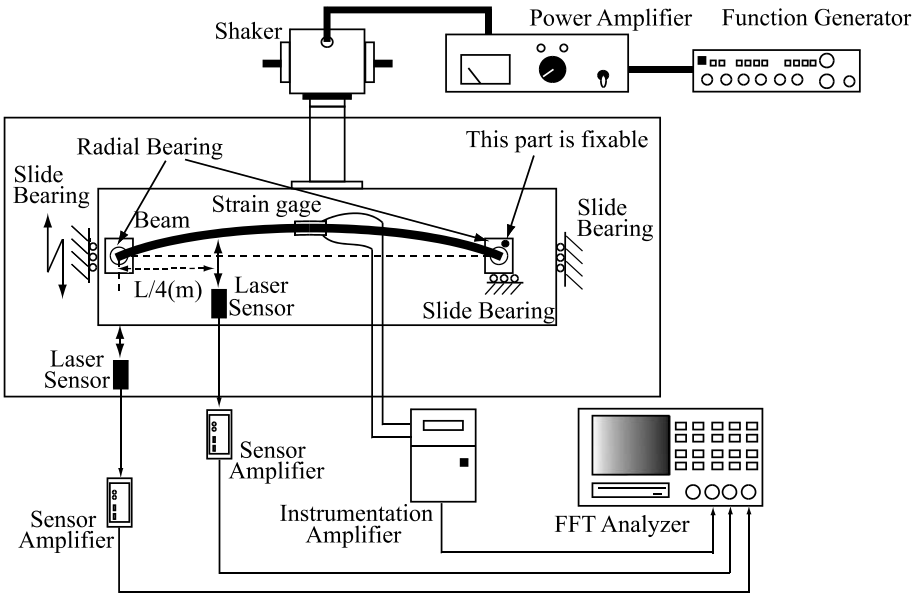

Fig. 6. A schematic view of the experimental setup.

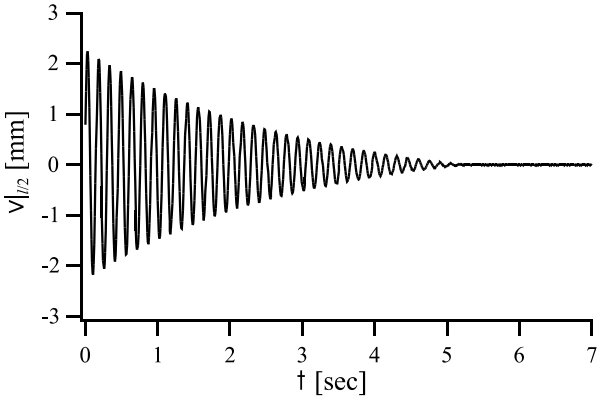

Fig. 7. Free decay of the first-mode response at the mid-span section toward the experimental estimation of the damping ratio.

indicates a possible premature jump due to the fact that, at high oscillation amplitudes on the upper resonant branch, the stable and unstable motions are very close and, hence, small perturbations, mostly caused by the excitation frequency step increments, are responsible for jumps onto the low-amplitude non-resonant motion whose basin of attraction is much larger than that of the large-amplitude attractor. These premature jumps cannot be easily avoided in spite of the great care exercised in performing the experiments. Each complete frequency sweep took on the average about ten hours. The overall shown agreement clearly denotes the high fidelity of the proposed theory.

Subsequently, we interrogated the simply supported (axially unrestrained) beam with the same excitation conditions as those in Fig. 4 ($Y_b = 0.5$ mm). The boundary mass of the sliding bearing is $m_\ell = 0.250$ kg ($\mu = 8.1$). The experimentally obtained frequency–response is shown superimposed on that theoretically

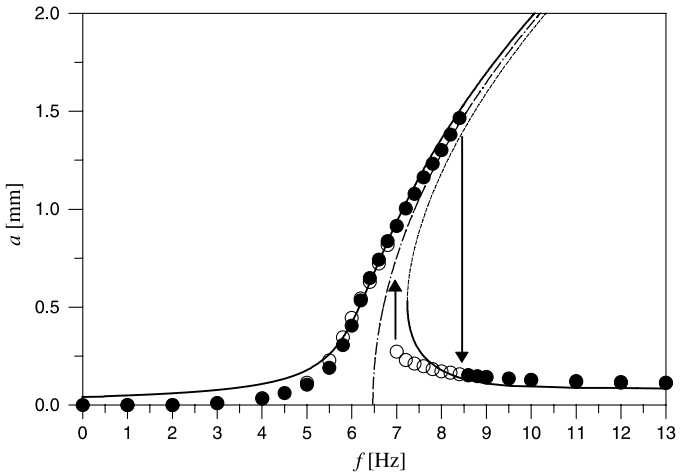

Fig. 8. Experimentally (circles) and theoretically (solid lines) obtained frequency–response curves of the first mode of the hinged–hinged test beam when $Y_b = 0.017$ mm. Filled (unfilled) circles indicate forward (backward) sweeps. The dashed-dotted line indicates the theoretical backbone.

predicated in Fig. 9. The agreement between the theoretical predictions and the experimental results is good. To further corroborate the findings and the repeatability of the experiments, using a different setup, three frequency–response curves were measured for three increasingly higher excitation amplitudes as shown in Fig. 10. In this case, the high-resolution sensor was used to measure the transverse displacement of the beam at its quarter-span section from left. The results indicate that, as expected, the frequency–response curves are of the softening type regardless of the excitation amplitude; further, the width of the multi-valued frequency range increases with the excitation amplitude as theoretically predicted in Fig. 4.

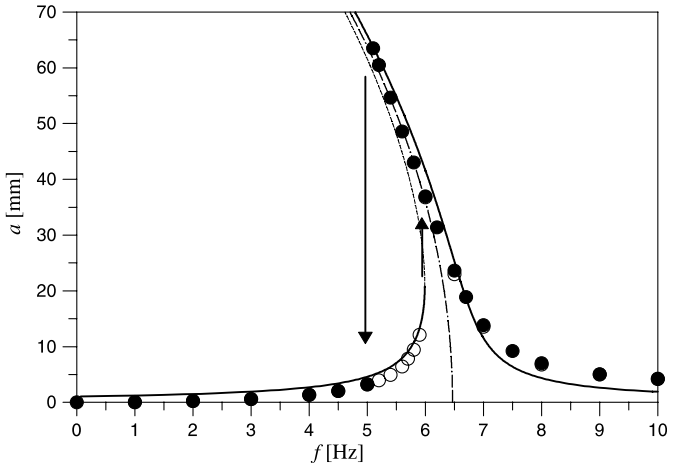

Fig. 9. Experimentally (circles) and theoretically (solid lines) obtained frequency–response curves of the first mode of the simply supported test beam when $a_b = 0.5$ mm. Filled (unfilled) circles indicate backward (forward) sweeps. The dashed-dotted line indicates the theoretical backbone.

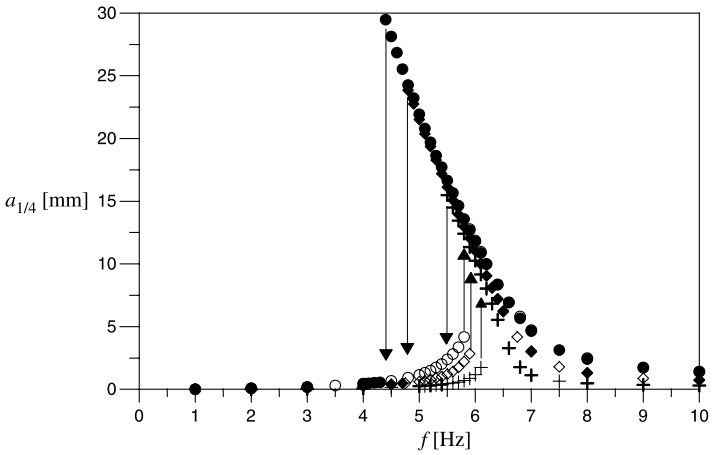

Fig. 10. Experimentally obtained (circles) frequency–response curves of the first mode of the simply supported test beam when $a_b = 0.2$ mm (crosses), $a_b = 0.5$ mm (diamonds), and $a_b = 0.85$ mm (circles). Filled (unfilled) symbols indicate backward (forward) sweeps and $a|_{1/4}$ indicates the displacement amplitude of the quarter-span beam section.

7. Conclusions

Three models of straight non-uniform beams undergoing large in-plane motions have been proposed, all derived from the geometrically exact theory of rods. The most general and relaxed model describes extensional and bending motions and neglects shear deformations; hence, it is suitable to predict nonlinear motions of slender beams with general boundary conditions. The second model is a constrained version of the previous one whereby, using asymptotic arguments, the longitudinal motion is expressed in terms of the leading transverse motion. The third model, incorporating the inextensibility and unshearability constraints, describes bending motions only; hence, it is suitable for beams that are either axially unrestrained or weakly restrained.

For all beam models, the order-three expanded equations of motion have been determined in a form amenable to a perturbation treatment. These equations have also been obtained using Hamilton's extended principle based on a rigorously truncated kinematic model. Closed-form solutions of the responses to primary resonances of the bending modes have been determined employing the method of multiple scales directly applied to the governing equations of motion. The solutions have been compared with the predictions of literature models in nonlinear beam theory. It has been ascertained that, for axially restrained beams, the model due to Mettler is an asymptotic expansion of the richer and more relaxed models here presented that allow to capture more accurately the strain field, hence the stretching effect, as well as contributions from the longitudinal motion. Moreover, for axially unrestrained beams (here, simply supported beams), it is confirmed, as pointed out by previous studies, that the inertia nonlinearity dictates the softening signature of the first-mode vibrations. However, comparisons with the predictions of an existing approximate theory show that the latter overestimates the effective nonlinearity coefficient of the mode, hence the nonlinear strength of the first-mode motions.

The fidelity of the proposed models has been assessed comparing the theoretically obtained frequency–response curves of the first mode of two test beams with those experimentally obtained. The proposed refined models may also be suitable to describe general classes of in-plane motions of non-uniform micro-beams subject to different loading and boundary conditions.

Acknowledgement

The help with some of the experiments by Miss Haruna Okamoto and Mr Koji Tsumoto is gratefully acknowledged. This work was supported by Grants-in-Aid for Scientific Research of the Japanese Ministry of Education, Culture, Sports, Science, and Technology, No. 15360222.

References

Atluri, S., 1973. Nonlinear vibrations of a hinged beam including nonlinear inertia effects. J. Appl. Mech. 40, 121–126.

Crespo da Silva, M.R.M., 1988. Nonlinear flexural–flexural-torsional-extensional dynamics of beams-II. Response analysis. Int. J. Solids Struct. 24, 1235–1242.

Crespo da Silva, M.R.M., Glynn, C.V.C., 1978. Nonlinear flexural–flexural-torsional dynamics of inextensional beams I. Equations of motion. J. Struct. Mech. 6, 437–448.

Eisley, J.G., 1964. Nonlinear vibration of beams and rectangular plates. Z. Angew. Math. Phys. 15, 167–175.

Gattulli, V., Martinelli, L., Perotti, F., Vestroni, F., 2004. Nonlinear oscillations of cables under harmonic loading using analytical and finite element models. Comput. Method Appl. Mech. 193, 69–85.

Lacarbonara, W., 1999. Direct treatment and discretizations of nonlinear spatially continuous systems. J. Sound Vib. 221, 849–866.

Lacarbonara, W., Camillacci, R., 2004. Nonlinear normal modes of structural systems via asymptotic approach. Int. J. Solids Struct. 41, 5565–5594.

Lacarbonara, W., Paolone, A., Yabuno, H., 2004. Modeling of planar nonshallow prestressed beams towards asymptotic solutions. Mech. Res. Commun. 31, 301–310.

Luongo, A., Rega, G., Vestroni, F., 1986. On nonlinear dynamics of planar shear undeformable beams. J. Appl. Mech. 108, 619–624.

Mettler, E., 1962. Dynamic buckling. In: Flugge (Ed.), Handbook of Engineering Mechanics. McGraw-Hill, New York.

Nayfeh, A.H., Pai, P.F., 2004. Linear and Nonlinear Structural Mechanics. Wiley-Interscience, New York.

Nayfeh, A.H., Mook, D.T., Lobitz, D.W., 1974. Numerical-perturbation method for the nonlinear analysis of structural vibrations. AIAA J. 12, 1222–1228.

Villaggio, P., 1997. Mathematical Models for Elastic Structures. Cambridge University Press.